

Rhenium(VII) Oxo–Alkyl Complexes: Reductive and α -Elimination Reactions

Shiang Cai,^{1a} David M. Hoffman,^{*,1b} and Derk A. Wierda^{1a,c}

Departments of Chemistry, University of Houston, Houston, Texas 77204, and
Harvard University, Cambridge, Massachusetts 02138.

Received September 25, 1995[®]

Alkylation of $\text{ReO}_2(\text{CH}_2\text{CMe}_3)_2\text{X}(\text{py})$ ($\text{X} = \text{Cl}, \text{Br}$) with ZnR_2 at low temperature gives $\text{ReO}_2(\text{CH}_2\text{CMe}_3)_2\text{R}$ ($\text{R} = \text{Me}, \text{CH}_2\text{CMe}_3, \text{CH}_2\text{SiMe}_3, \text{Ph}$) in high yield. The crystal structure of $\text{ReO}_2(\text{CH}_2\text{CMe}_3)_2\text{Ph}$ shows that it has a distorted trigonal bipyramidal structure with the oxo and Ph ligands in the equatorial plane. Photolysis of $\text{ReO}_2(\text{CH}_2\text{CMe}_3)_3$ in pyridine gives neopentane and $\text{ReO}_2(\text{CHCMe}_3)(\text{CH}_2\text{CMe}_3)$, and $\text{ReO}_2(\text{CHCMe}_3)(\text{CH}_2\text{CMe}_3)$ reacts with quinuclidine to give $\text{ReO}_2(\text{CHCMe}_3)(\text{CH}_2\text{CMe}_3)(\text{quinuclidine})$. In the solid state, $\text{ReO}_2(\text{CHCMe}_3)(\text{CH}_2\text{CMe}_3)$ has a distorted tetrahedral structure, and $\text{ReO}_2(\text{CHCMe}_3)(\text{CH}_2\text{CMe}_3)(\text{quinuclidine})$ is trigonal bipyramidal with the neopentylidene and oxo ligands defining the equatorial plane. The Re–N bond distance is long, suggesting the rhenium–quinuclidine interaction is weak. Thermolysis of $\text{ReO}_2(\text{CH}_2\text{CMe}_3)_2\text{Ph}$ in pyridine gives $\text{ReO}_2(\text{CH}_2\text{CMe}_3)(\text{py})_3$ and neopentylbenzene. An X-ray structure of $\text{ReO}_2(\text{CH}_2\text{CMe}_3)(\text{py})_3$ shows that it is octahedral with trans oxo groups. In solution $\text{ReO}_2(\text{CH}_2\text{CMe}_3)(\text{py})_3$ is unstable in the absence of excess pyridine, and in the solid state it readily loses pyridine. $\text{ReO}_2(\text{CH}_2\text{CMe}_3)(\text{py})_3$ reacts with $\text{MeC}\equiv\text{CMe}$ and $\text{PhC}\equiv\text{CH}$ to form $\text{ReO}_2(\text{CH}_2\text{CMe}_3)(\text{alkyne})$ compounds.

There has recently been a renewed interest in the chemistry of high oxidation state rhenium compounds.² Herrmann and co-workers, for example, have comprehensively developed the chemistry of Cp^*ReO_3 and MeReO_3 , including the latter's use in catalytic olefin metathesis,³ aldehyde alkenation,⁴ and olefin epoxidation reactions,⁵ while Schrock and co-workers have advanced the chemistry of rhenium imido, alkylidene, and alkylidyne compounds culminating in the synthesis of well-characterized Re(VII) olefin and acetylene metathesis catalysts.⁶ Despite the interest in and the proven importance of Re(VII) organometallic complexes in catalytic processes, however, there are still relatively few^{7–10} Re(VII) organometallic oxo complexes other than Cp^*ReO_3 , MeReO_3 , and their derivatives.²

We recently reported that photolysis of $\text{ReO}_2(\text{CH}_2\text{CMe}_3)_3$ gives $\text{ReO}_2(\text{CHCMe}_3)(\text{CH}_2\text{CMe}_3)$, a rare example of a Re oxo alkylidene complex.^{8d} Motivated by this result, we were interested in preparing Re(VII) compounds analogous to $\text{ReO}_2(\text{CH}_2\text{CMe}_3)_3$ and examining their thermal and photolytic decomposition. We report here the synthesis of alkyl compounds of the type $\text{ReO}_2(\text{CH}_2\text{CMe}_3)_2\text{R}$, full details concerning the synthesis of $\text{ReO}_2(\text{CHCMe}_3)(\text{CH}_2\text{CMe}_3)$ and its quinuclidine adduct, and the thermolysis of $\text{ReO}_2(\text{CH}_2\text{CMe}_3)_2\text{Ph}$ to give reactive $\text{ReO}_2(\text{CH}_2\text{CMe}_3)(\text{py})_3$.

Results

Scheme 1 shows a brief summary of our synthetic results.

$\text{ReO}_2(\text{CH}_2\text{CMe}_3)_2\text{R}$. $\text{ReO}_2(\text{CH}_2\text{CMe}_3)_2\text{X}(\text{py})$ ($\text{X} = \text{Br}, \text{Cl}$),^{8b} prepared from $[\text{Re}(\mu\text{-O})\text{O}(\text{CH}_2\text{CMe}_3)_2]_2$,¹¹ reacts

[®] Abstract published in *Advance ACS Abstracts*, January 1, 1996.

(1) (a) Harvard University. Present address: Strem Chemicals, Inc., Newburyport, MA. (b) University of Houston. (c) Harvard University. Present address: Department of Chemistry, St. Anselm College, Manchester, NH.

(2) Hoffman, D. M. In *Comprehensive Organometallic Chemistry II*; Abel, E. W., Stone, F. G. A., Wilkinson, G., Eds.; Pergamon Press: New York, 1995; Vol. 6, Chapter 10.

(3) Herrmann, W. A.; Kuchler, J. G.; Felixberger, J. K.; Herdtweck, E.; Wagner, W. *Angew. Chem., Int. Ed. Engl.* **1988**, *27*, 394; *Angew. Chem.* **1988**, *100*, 420. Herrmann, W. A.; Wagner, W.; Flessner, U. N.; Volkhardt, U.; Kombar, H. *Angew. Chem., Int. Ed. Engl.* **1991**, *30*, 1636; *Angew. Chem.* **1991**, *103*, 1704.

(4) Herrmann, W. A.; Wang, M. *Angew. Chem., Int. Ed. Engl.* **1991**, *30*, 1641; *Angew. Chem.* **1991**, *103*, 1709.

(5) Herrmann, W. A.; Marz, D.; Wagner, W.; Kuchler, J.; Weichselbaumer, G.; Fischer, R. (Hoechst AG) Ger. Offen. DE 3,902,357, 1990; *Chem. Abstr.* **1991**, *114*, 143714u. Herrmann, W. A.; Fischer, R. W.; Marz, D. W. *Angew. Chem., Int. Ed. Engl.* **1991**, *30*, 1638; *Angew. Chem.* **1991**, *103*, 1706. Herrmann, W. A.; Fischer, R. W.; Scherer, W.; Rauch, M. U. *Angew. Chem., Int. Ed. Engl.* **1993**, *32*, 1157; *Angew. Chem.* **1993**, *105*, 1209.

(6) (a) Toreki, R.; Schrock, R. R. *J. Am. Chem. Soc.* **1990**, *112*, 2448. (b) Toreki, R.; Vaughan, G. A.; Schrock, R. R.; Davis, W. M. *J. Am. Chem. Soc.* **1993**, *115*, 127. (c) Schrock, R. R.; Weinstock, I. A.; Horton, A. D.; Liu, A. H.; Schofield, M. H. *J. Am. Chem. Soc.* **1988**, *110*, 2686. (d) Weinstock, I. A.; Schrock, R. R.; Davis, W. M. *J. Am. Chem. Soc.* **1991**, *113*, 135.

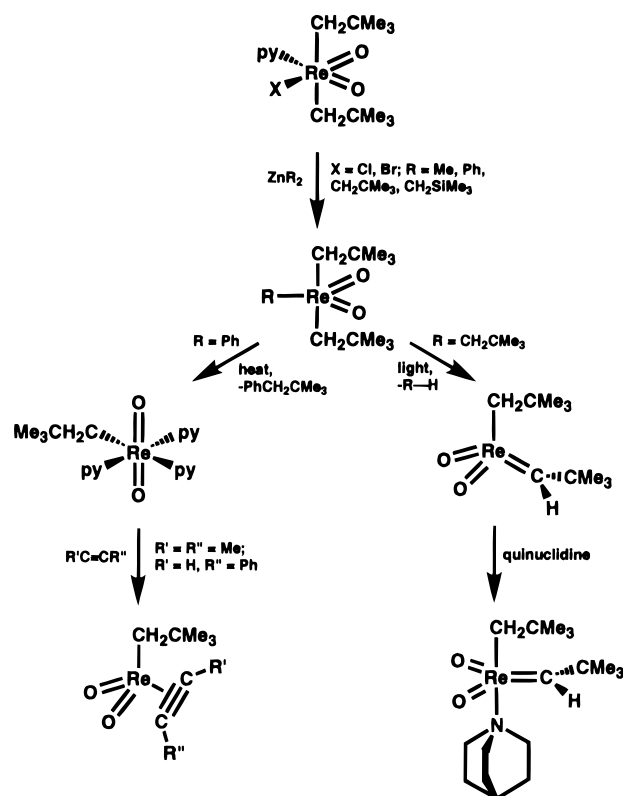
(7) Mertis, K.; Wilkinson, G. *J. Chem. Soc., Dalton Trans.* **1976**, 1488. Gutierrez, A.; Wilkinson, G.; Hussain-Bates, B.; Hursthouse, M. B. *Polyhedron* **1990**, *9*, 2081.

(8) (a) Cai, S.; Hoffman, D. M.; Lappas, D.; Woo, H.-G.; Huffman, J. C. *Organometallics* **1987**, *6*, 2273. (b) Cai, S.; Hoffman, D. M.; Wierda, D. A. *Organometallics* **1988**, *7*, 2069. (c) Cai, S.; Hoffman, D. M.; Wierda, D. A. *J. Chem. Soc., Chem. Commun.* **1988**, 313. (d) Cai, S.; Hoffman, D. M.; Wierda, D. A. *J. Chem. Soc., Chem. Commun.* **1988**, 1489. (e) Cai, S.; Hoffman, D. M.; Wierda, D. A. *Inorg. Chem.* **1989**, *28*, 3784.

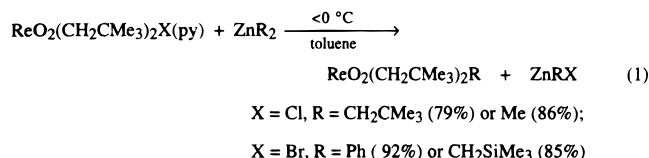
(9) (a) Takacs, J.; Kiprof, P.; Riede, J.; Herrmann, W. A. *Organometallics* **1990**, *9*, 782. (b) Takacs, J.; Cook, M. R.; Kiprof, P.; Kuchler, J. G.; Herrmann, W. A. *Organometallics* **1991**, *10*, 316. (c) Herrmann, W. A.; Watzlowik, P.; Kiprof, P. *Chem. Ber.* **1991**, *124*, 1101. (d) Herrmann, W. A.; Watzlowik, P. *J. Organomet. Chem.* **1992**, *441*, 265. (e) Herrmann, W. A.; Weichselbaumer, G.; Paciello, R. A.; Fischer, R. A.; Herdtweck, E.; Okuda, J.; Marz, D. W. *Organometallics* **1990**, *9*, 489. (f) Takacs, J.; Kiprof, P.; Kuchler, J. G.; Herrmann, W. A. *J. Organomet. Chem.* **1989**, *369*, C1.

(10) Horton, A. D.; Schrock, R. R. *Polyhedron* **1988**, *7*, 1841. Horton, A. D.; Schrock, R. R.; Freudenberger, J. H. *Organometallics* **1987**, *6*, 893. Toreki, R.; Schrock, R. R.; Davis, W. M. *J. Am. Chem. Soc.* **1992**, *114*, 3367.

Scheme 1



with dialkylzinc reagents at low temperature to give $\text{ReO}_2(\text{CH}_2\text{CMe}_3)_2\text{R}$ compounds in high yield (eq 1). For



the phenyl and trimethylsilylmethyl derivatives, work-up of the reaction mixtures included treatment with oxygen-free water to destroy unreacted dialkylzinc reagents and ZnRX . Final isolation of the compounds as orange solids was accomplished by vacuum sublimation. The compounds are very soluble in hydrocarbon solvents. They are stable to oxygen-free water but are light and thermally sensitive. The preparation of $\text{ReO}_2(\text{CH}_2\text{CMe}_3)_3$ from $\text{ReO}_2(\text{CH}_2\text{CMe}_3)_2\text{X}(\text{py})$ and $\text{Zn}(\text{CH}_2\text{CMe}_3)_2$ (eq 1) is a more convenient synthesis than the previously reported one.^{8c}

The structure of $\text{ReO}_2(\text{CH}_2\text{CMe}_3)_2\text{Ph}$ was determined by X-ray crystallography. A thermal ellipsoid plot is presented in Figure 1, and selected bond distances and angles are given in Table 1. The ReO_2C_3 core can be described as distorted trigonal bipyramidal with the plane defined by Re , $\text{O}(1)$, $\text{O}(2)$, and $\text{C}(3)$ of the phenyl ring taken as the equatorial plane. The axial neopentyl methylene carbons, $\text{C}(1)$ and $\text{C}(2)$, bend in the direction of the phenyl ligand giving an angle of $145.4(2)^\circ$ for $\text{C}(1)-\text{Re}-\text{C}(2)$. The bending of *cis* ligands away from the oxo groups is a common feature for d^0 *cis*-dioxo compounds.

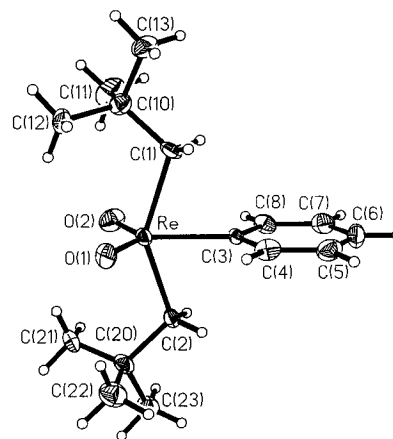


Figure 1. Plot of $\text{ReO}_2(\text{CH}_2\text{CMe}_3)_2\text{Ph}$ showing the atom numbering scheme (30% probability level ellipsoids).

Table 1. Selected Bond Distances (Å) and Angles (deg) for $\text{ReO}_2(\text{CH}_2\text{CMe}_3)_2\text{Ph}$

Distances			
Re—O(1)	1.709(6)	Re—O(2)	1.704(5)
Re—C(1)	2.163(8)	Re—C(2)	2.152(7)
Re—C(3)	2.142(6)		
Angles			
O(1)—Re—O(2)	123.8(2)	C(1)—Re—C(2)	145.4(2)
O(1)—Re—C(1)	98.6(3)	C(1)—Re—C(3)	72.5(2)
O(2)—Re—C(1)	97.3(3)	C(2)—Re—C(3)	73.1(2)
O(1)—Re—C(2)	99.9(3)	Re—C(1)—C(10)	114.0(5)
O(2)—Re—C(2)	96.3(2)	Re—C(2)—C(20)	114.4(4)
O(1)—Re—C(3)	117.0(2)	Re—C(3)—C(4)	119.2(5)
O(2)—Re—C(3)	119.2(3)	Re—C(3)—C(8)	122.3(4)

The $\text{O}(2)-\text{Re}-\text{O}(1)$ angle ($123.8(2)^\circ$) in $\text{ReO}_2(\text{CH}_2\text{CMe}_3)_2\text{Ph}$ is larger than the $\text{O}-\text{Re}-\text{O}$ angles in octahedral $\text{ReO}_2(\text{CH}_2\text{CMe}_3)_2\text{Br}(\text{py})$ ($107.4(3)^\circ$)^{8b} and the 5-coordinate compounds $\text{ReO}_2(\text{CH}_2\text{CMe}_3)_3$ ($117.4(5)^\circ$), $[\text{ReO}_2(\text{CH}_2\text{CMe}_3)_2]_2(\mu\text{-O})$ ($107.5(6)^\circ$ (av)), and $\text{ReO}_2(\text{CH}_2\text{CMe}_3)_2(\text{SPh})$ ($117.7(3)^\circ$).^{8c,e} The $\text{Re}-\text{O}$ and $\text{Re}-\text{C}$ distances in $\text{ReO}_2(\text{CH}_2\text{CMe}_3)_2\text{Ph}$ are normal, and the neopentyl and phenyl $\text{Re}-\text{C}$ distances are within 3σ of each other.

IR spectra for the $\text{ReO}_2(\text{CH}_2\text{CMe}_3)_2\text{R}$ compounds show two bands in the region $940-1000\text{ cm}^{-1}$ (e.g., $\text{R} = \text{Ph}$, 987 and 945 cm^{-1}) that are characteristic of the symmetric and antisymmetric stretches arising from a *cis*- ReO_2 fragment.¹²

Consistent with the solid-state structure of $\text{ReO}_2(\text{CH}_2\text{CMe}_3)_2\text{Ph}$, room-temperature ^1H NMR spectra for the $\text{ReO}_2(\text{CH}_2\text{CMe}_3)_2\text{R}$ compounds show only a singlet for the neopentyl methylene protons, indicating that the neopentyl ligands occupy axial sites. Variable-temperature NMR spectra recorded for $\text{ReO}_2(\text{CH}_2\text{CMe}_3)_2\text{Ph}$ ($+23$ to -90°C) are consistent with the solid-state structure being retained in solution over the entire temperature range. Spectra recorded for $\text{ReO}_2(\text{CH}_2\text{CMe}_3)_2\text{Me}$ in the same temperature range are also invariant.

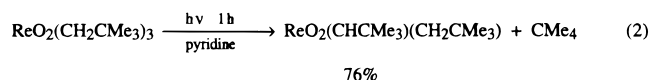
In contrast, ^1H NMR spectra recorded for $\text{ReO}_2(\text{CH}_2\text{CMe}_3)_2(\text{CH}_2\text{SiMe}_3)$ display a temperature dependence. As the sample is cooled, the resonance arising from the axial methylene protons (CH_2CMe_3) broadens, then collapses into the baseline (at -65°C), and finally reappears as an AB quartet (-86°C). The singlet

(11) Cai, S.; Hoffman, D. M.; Huffman, J. C.; Wierda, D. A.; Woo, H.-G. *Inorg. Chem.* **1987**, *26*, 3693. Huggins, J. M.; Whitt, D. R.; Lebiada, L. *J. Organomet. Chem.* **1986**, *312*, C15.

(12) Nakamoto, K. *Infrared and Raman Spectra of Inorganic and Coordination Compounds*, 4th ed.; John Wiley & Sons: New York, 1986.

arising from the equatorial methylene protons ($\text{CH}_2\text{-SiMe}_3$) broadens slightly as the sample is gradually cooled, but it never disappears into the baseline. The low-temperature-limiting ^1H NMR spectrum of $\text{ReO}_2(\text{CH}_2\text{CMe}_3)_2(\text{CH}_2\text{SiMe}_3)$ closely resembles the limiting spectra of $\text{ReO}_2(\text{CH}_2\text{SiMe}_3)_3$ and $\text{ReO}_2(\text{CH}_2\text{CMe}_3)_3$,^{8c} the latter having a highly distorted *tbp* structure in the solid state in which the methylene groups lean toward one of the oxo ligands. Thus, the NMR data suggest that $\text{ReO}_2(\text{CH}_2\text{CMe}_3)_2(\text{CH}_2\text{SiMe}_3)$ also has a distorted geometry in the low-temperature limit. The temperature-independent spectra observed for $\text{ReO}_2(\text{CH}_2\text{CMe}_3)_2\text{Me}$ could mean it adopts the undistorted $\text{ReO}_2(\text{CH}_2\text{CMe}_3)_2\text{-Ph}$ structure or that we simply could not freeze out the pathway that generates virtual C_{2v} symmetry in the molecule. The lesser steric crowding in $\text{ReO}_2(\text{CH}_2\text{CMe}_3)_2\text{Me}$ compared to the other alkyl derivatives could be the basis for either explanation.

$\text{ReO}_2(\text{CHCMe}_3)(\text{CH}_2\text{CMe}_3)$ and $\text{ReO}_2(\text{CHCMe}_3)(\text{CH}_2\text{CMe}_3)(\text{quin})$. Photolysis of $\text{ReO}_2(\text{CH}_2\text{CMe}_3)_3$ in pyridine for 1 h using Pyrex-filtered light from a medium-pressure mercury lamp gives $\text{ReO}_2(\text{CHCMe}_3)(\text{CH}_2\text{CMe}_3)$ and neopentane as the only identifiable products (eq 2). Acetonitrile can also be used



as a solvent for the photolysis reaction, but photolysis in hydrocarbon solvents gives a mixture of $\text{ReO}_2(\text{CHCMe}_3)(\text{CH}_2\text{CMe}_3)$ and $\text{Re(VI)} [\text{Re}(\mu\text{-O})\text{O}(\text{CH}_2\text{CMe}_3)_2]_2$.¹¹ A possible explanation for the solvent dependence is that coordinating solvents weakly associate with $\text{ReO}_2(\text{CH}_2\text{CMe}_3)_3$, thereby increasing steric congestion and facilitating α -hydrogen elimination.

$\text{ReO}_2(\text{CHCMe}_3)(\text{CH}_2\text{CMe}_3)$ does not react under mild conditions with cyclic or acyclic olefins or alkynes. Since coordination of olefin or alkyne is a likely prerequisite for reactivity with $\text{ReO}_2(\text{CHCMe}_3)(\text{CH}_2\text{CMe}_3)$, we reacted the alkylidene complex with quinuclidine to determine if an adduct could be formed with a strong donor ligand. Thus, the addition of quinuclidine to the crude reaction mixture from (2) gave yellow $\text{ReO}_2(\text{CHCMe}_3)(\text{CH}_2\text{CMe}_3)(\text{quin})$ (quin = quinuclidine), which was isolated in 54% yield based on $\text{ReO}_2(\text{CH}_2\text{CMe}_3)_3$ after crystallization from acetonitrile.

$\text{ReO}_2(\text{CHCMe}_3)(\text{CH}_2\text{CMe}_3)$ and $\text{ReO}_2(\text{CHCMe}_3)(\text{CH}_2\text{CMe}_3)(\text{quin})$ are very soluble in common solvents, and both are moderately air-stable in the solid state and in solution. $\text{ReO}_2(\text{CHCMe}_3)(\text{CH}_2\text{CMe}_3)$ sublimes readily under vacuum.

$\text{ReO}_2(\text{CHCMe}_3)(\text{CH}_2\text{CMe}_3)$ (Figure 2) and $\text{ReO}_2(\text{CHCMe}_3)(\text{CH}_2\text{CMe}_3)(\text{quin})$ (Figure 3) were characterized by X-ray crystallography. Selected bond distances and angles are given in Tables 2 and 3.

Judging by the 3σ criterion, there is no significant difference in the $\text{Re}=\text{C}(1)$ or $\text{Re}-\text{O}$ distances between the two complexes. Also, the $\text{Re}=\text{C}$ distances (1.869(9) and 1.893(6) Å) are close to those reported for $\text{Re}(\text{CCMe}_3)(\text{CHCMe}_3)\text{I}_2(\text{py})_2$ (1.873(9) Å),¹³ $[\text{Re}(\text{CCMe}_3)(\text{CHCMe}_3)(\text{ArNH}_2)\text{Cl}_2]_2$ (1.89(1) Å),^{6a} and $\text{Re}(\text{CHCMe}_3)(\text{N-2,6-C}_6\text{H}_3\text{-}i\text{-Pr}_2)(\text{O-2,6-C}_6\text{H}_3\text{Cl}_2)_3$ (1.87(2) Å),¹⁴ and

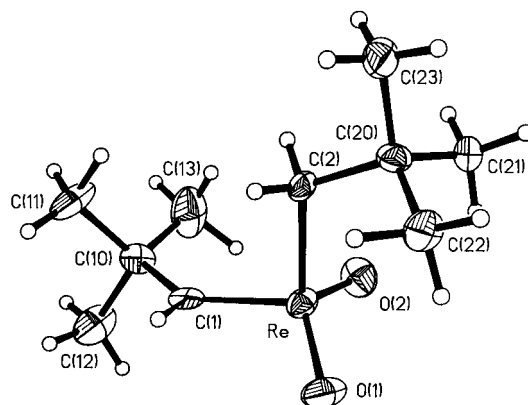


Figure 2. Plot of $\text{ReO}_2(\text{CHCMe}_3)(\text{CH}_2\text{CMe}_3)$ showing the atom-numbering scheme (30% probability level ellipsoids).

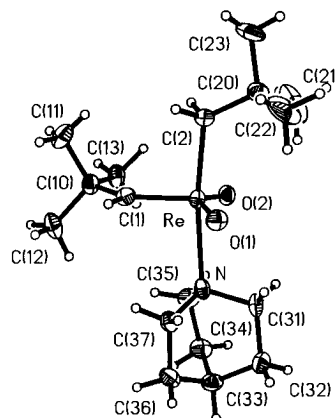


Figure 3. Plot of $\text{ReO}_2(\text{CHCMe}_3)(\text{CH}_2\text{CMe}_3)(\text{quin})$ showing the atom-numbering scheme (30% probability level ellipsoids).

Table 2. Selected Bond Distances (Å) and Angles (deg) for $\text{ReO}_2(\text{CHCMe}_3)(\text{CH}_2\text{CMe}_3)$

Distances			
Re-O(2)	1.696(7)	Re-C(2)	2.114(9)
Re-O(1)	1.706(7)	Re-C(1)	1.869(9)
C(1)-C(10)	1.501(13)	C(2)-C(20)	1.558(13)
Angles			
O(2)-Re-O(1)	124.6(4)	O(1)-Re-C(1)	109.3(4)
O(2)-Re-C(2)	105.0(4)	C(2)-Re-C(1)	94.8(4)
O(1)-Re-C(2)	106.9(3)	Re-C(2)-C(20)	117.4(6)
O(2)-Re-C(1)	111.7(4)	Re-C(1)-C(10)	136.6(8)

Table 3. Selected Bond Distances (Å) and Angles (deg) for $\text{ReO}_2(\text{CHCMe}_3)(\text{CH}_2\text{CMe}_3)(\text{quin})$

Distances			
Re-O(1)	1.718(4)	Re-N	2.425(5)
Re-O(2)	1.722(4)	C(1)-C(10)	1.494(8)
Re-C(1)	1.893(6)	C(2)-C(20)	1.540(9)
Re-C(2)	2.144(7)		
Angles			
O(1)-Re-O(2)	133.3(2)	O(1)-Re-N	81.5(2)
O(1)-Re-C(1)	110.8(2)	O(2)-Re-N	82.3(2)
O(2)-Re-C(1)	113.9(2)	C(1)-Re-N	94.2(2)
O(1)-Re-C(2)	95.6(2)	C(2)-Re-N	172.0(2)
O(2)-Re-C(2)	94.5(2)	Re-C(1)-C(10)	136.8(4)
C(1)-Re-C(2)	93.8(3)	Re-C(2)-C(20)	120.5(4)

the $\text{Re}-\text{O}$ distances (1.70–1.72 Å) are normal. The $\text{Re}=\text{C}_\alpha\text{-C}_\beta$ angles in both complexes ($\approx 137^\circ$) are about 14° smaller than the angle observed in $\text{Re}(\text{CCMe}_3)(\text{CHCMe}_3)\text{I}_2(\text{py})_2$,¹³ but they are close to those observed

(13) Edwards, D. S.; Biondi, L. V.; Ziller, J. W.; Churchill, M. R.; Schrock, R. R. *Organometallics* **1983**, *2*, 1505.

(14) Schofield, M. H.; Schrock, R. R.; Park, L. Y. *Organometallics* **1991**, *10*, 1844.

in $[\text{Re}(\text{CCMe}_3)(\text{CHCMe}_3)(\text{ArNH}_2)\text{Cl}_2]_2$ (140(1)°) and $\text{Re}(\text{CHCMe}_3)(\text{N}-2,6\text{-C}_6\text{H}_3\text{-}i\text{Pr}_2)(\text{O}-2,6\text{-C}_6\text{H}_3\text{Cl}_2)_3$ (139(1)°).^{6a,14} Undistorted alkylidene ligands are usually found in compounds in which there are strong π -donating ligands, such as oxo and imido groups. The Re–N bond distance (2.425(5) Å) in $\text{ReO}_2(\text{CHCMe}_3)(\text{CH}_2\text{CMe}_3)(\text{quin})$ is comparable to the Re–N distances in other complexes in which the amine ligand is trans to an alkyl group, such as $\text{ReO}_3(\text{Me})(\text{NH}_2\text{Ph})$ (2.469(4) Å),¹⁵ $\text{ReO}_2(\text{Me})(\text{py})(1,2\text{-O}_2\text{C}_6\text{H}_4)$ (2.347(4) Å),^{9a} and $\text{ReO}_3\text{R}(\text{quin})$ (R = Et, $\text{CH}_2\text{-SiMe}_3$, CH_2CMe_3 , cyclopropyl; av Re–N = 2.41 Å).¹⁶ A normal Re–N distance is around 2.1–2.2 Å (see the next section).

The ReO_2C_2 core of $\text{ReO}_2(\text{CHCMe}_3)(\text{CH}_2\text{CMe}_3)$ has a distorted tetrahedral geometry. The C(2)–Re–O(1) and C(2)–Re–O(2) angles (106.9(3) and 105.0(4)°) are close to the expected tetrahedral values, but the C(1)–Re–C(2) angle is only 94.8 (4)° and O(1)–Re–O(2) is 124.6(4)°. The geometry about the rhenium in $\text{ReO}_2(\text{CHCMe}_3)(\text{CH}_2\text{CMe}_3)(\text{quin})$ is trigonal bipyramidal with the oxo and neopentylidene ligands defining the trigonal plane and the quinuclidine and neopentyl ligands occupying the axial positions. The axial ligands are slightly bent away from the bulky neopentylidene ligand. The rhenium, neopentylidene α carbon, and two oxo ligands are nearly coplanar, but the O–Re–C(1) angles are smaller (by 6 and 10°) than 120° as a consequence of the large O–Re–O angle of 133°. The O–Re–O angles in $\text{ReO}_2(\text{CHCMe}_3)(\text{CH}_2\text{CMe}_3)$ (125°) and its quinuclidine adduct (133°) are larger than those found in the related complexes ReO_3R (107–112°)¹⁷ and $\text{ReO}_3\text{R}(\text{amine})$ (115–120°).^{15,16}

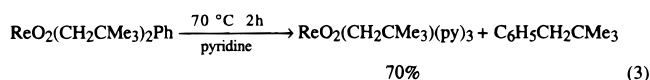
Spectroscopic data for $\text{ReO}_2(\text{CHCMe}_3)(\text{CH}_2\text{CMe}_3)$ and $\text{ReO}_2(\text{CHCMe}_3)(\text{CH}_2\text{CMe}_3)(\text{quin})$ are consistent with the solid-state structures. In particular, the methylene protons of the neopentyl alkyl ligand in each compound appears as a sharp AB quartet in the ^1H NMR spectra, indicating that the neopentylidene plane is perpendicular to the Re– CH_2CMe_3 bond vector in solution and the neopentylidene ligand does not rotate rapidly enough to broaden the NMR signals. The IR spectrum for $\text{ReO}_2(\text{CHCMe}_3)(\text{CH}_2\text{CMe}_3)$ has strong bands at 986 and 947 cm^{-1} arising from the *cis*- ReO_2 moiety.¹² Similar bands appear in the spectrum of the quinuclidine adduct, but both are shifted to lower energy by $\approx 40\text{--}50\text{ cm}^{-1}$. Assuming an 18-electron count for $\text{ReO}_2(\text{CHCMe}_3)(\text{CH}_2\text{CMe}_3)$ and $\text{ReO}_2(\text{CHCMe}_3)(\text{CH}_2\text{CMe}_3)(\text{quin})$, the predicted Re–O bond orders are 3 for $\text{ReO}_2(\text{CHCMe}_3)(\text{CH}_2\text{CMe}_3)$ and $2\frac{1}{2}$ for the quin adduct, consistent with the lower energy Re–O stretching bands observed for the quinuclidine adduct. For comparison, the Re–O stretching frequencies in ReO_3R (Re–O bond order $2\frac{2}{3}$) and $\text{ReO}_3\text{R}(\text{quin})$ (Re–O bond order $2\frac{1}{3}$) are ≈ 955 and $\approx 920\text{ cm}^{-1}$, respectively.^{16,17}

$\text{ReO}_2(\text{CH}_2\text{CMe}_3)(\text{py})_3$. Photolysis of $\text{ReO}_2(\text{CH}_2\text{CMe}_3)_2\text{R}$, R = Me or CH_2SiMe_3 , under conditions similar to those used to prepare $\text{ReO}_2(\text{CHCMe}_3)(\text{CH}_2\text{CMe}_3)$, gives $\text{ReO}_2(\text{CHCMe}_3)(\text{CH}_2\text{CMe}_3)$ as the only identifiable

Table 4. Selected Bond Distances (Å) and Angles (deg) for $\text{ReO}_2(\text{CH}_2\text{CMe}_3)(\text{py})_3$

Distances			
Re–O(1)	1.748(9)	Re–N(3)	2.158(11)
Re–O(2)	1.741(9)	Re–C(4A)	2.171(14)
Re–N(1)	2.348(11)	Re–C(4B)	2.187(19)
Re–N(2)	2.136(11)		
Angles			
O(1)–Re–O(2)	165.9(5)	N(1)–Re–N(3)	84.1(4)
O(1)–Re–N(1)	82.7(5)	N(2)–Re–N(3)	176.6(4)
O(2)–Re–N(1)	83.3(4)	N(1)–Re–N(2)	92.4(4)
O(1)–Re–N(2)	89.6(5)	O(1)–Re–N(3)	89.9(4)
O(2)–Re–N(2)	90.3(5)	O(2)–Re–N(3)	89.4(4)
O(1)–Re–C(4A)	103.1(7)	O(1)–Re–C(4B)	84.9(7)
O(2)–Re–C(4A)	90.8(7)	O(2)–Re–C(4B)	109.1(7)
N(1)–Re–C(4A)	171.6(7)	N(1)–Re–C(4B)	165.2(8)
N(2)–Re–C(4A)	81.5(5)	N(2)–Re–C(4B)	95.4(9)
N(3)–Re–C(4A)	101.9(5)	N(3)–Re–C(4B)	87.9(9)
Re–C(4A)–C(40)	129.9(11)	Re–C(4B)–C(40)	127.2(15)

alkylidene product by ^1H NMR. In contrast, photolysis of $\text{ReO}_2(\text{CH}_2\text{CMe}_3)_2\text{Ph}$ produces a mixture of products that includes $\text{Re(V)}\text{ReO}_2(\text{CH}_2\text{CMe}_3)(\text{py})_3$ and neopentylbenzene (identified by ^1H NMR). Subsequently, it was found that thermolysis of $\text{ReO}_2(\text{CH}_2\text{CMe}_3)_2\text{Ph}$ at 70 °C in pyridine gives $\text{ReO}_2(\text{CH}_2\text{CMe}_3)(\text{py})_3$ more cleanly than the photolysis route (eq 3).



$\text{ReO}_2(\text{CH}_2\text{CMe}_3)(\text{py})_3$ crystallizes from saturated pyridine solutions at low temperature. The crystals must be dried in vacuo at low temperature for a short time period, or under ambient conditions in a glovebox, to keep the three pyridine ligands intact. Under dynamic vacuum a for 12 h at room temperature a compound with a stoichiometry close to $\text{ReO}(\text{CH}_2\text{CMe}_3)(\text{py})_2$ (determined by ^1H NMR) is obtained.

$\text{ReO}_2(\text{CH}_2\text{CMe}_3)(\text{py})_x$ ($x < 3$) decomposes within a few minutes at room temperature in common organic solvents unless there is excess pyridine present. The decomposition products could not be identified. Attempts to prepare $\text{ReO}_2(\text{CH}_2\text{CMe}_3)(\text{py})_x$ from $[\text{ReO}_2(\text{py})_4]\text{Cl}$ and $\text{LiCH}_2\text{CMe}_3$ were unsuccessful.

$\text{ReO}_2(\text{CH}_2\text{CMe}_3)(\text{py})_3$ was characterized by X-ray crystallography. Selected bond distances and angles are presented in Table 4. In the course of solving the structure it was found that the neopentyl group is disordered. The thermal ellipsoid plot in Figure 4 shows one of the two resolved components of the disorder.

The coordination geometry about the rhenium is best described as octahedral. The oxo ligands are trans but they are slightly bent ($\angle\text{O–Re–O} = 165.9(5)^\circ$) in the direction of N(1). Generally, d^2 dioxo compounds have a trans rather than a cis configuration. The Re–O distances [average 1.745(9) Å] are similar to those in $[\text{ReO}_2(\text{py})_4]^+$ and other Re(V) *trans*-dioxo compounds,¹⁸ all of which are best described as having Re–O double bonds. The Re–C–C angles in the Re neopentyl group appear to be $\approx 5\text{--}10^\circ$ larger than normal (molecule A,

(15) Herrmann, W. A.; Weichselbaumer, G.; Herdtweck, E. *J. Organomet. Chem.* **1989**, 372, 371.

(16) Herrmann, W. A.; Romão, C. C.; Fischer, R. W.; Kiprof, P.; de Méric de Bellefon, C. *Angew. Chem., Int. Ed. Engl.* **1991**, 30, 185; *Angew. Chem.* **1991**, 103, 183. Herrmann, W. A.; Kühn, F. E.; Romão, C. C.; Huy, H. T.; Wang, M.; Fischer, R. W.; Kiprof, P.; Scherer, W. *Chem. Ber.* **1993**, 126, 45.

(17) de Méric de Bellefon, C.; Herrmann, W. A.; Kiprof, P.; Whitaker, C. R. *Organometallics* **1992**, 11, 1072.

(18) (a) Johnson, J. W.; Brody, J. F.; Ansell, G. B.; Zentz, S. *Inorg. Chem.* **1984**, 23, 2415. (b) Calvo, C.; Krishnamachari, N.; Lock, C. J. L. *J. Cryst. Mol. Struct.* **1971**, 1, 161. Lock, C. J. L.; Turner, G. *Acta Crystallogr.* **1978**, B34, 923. (c) Edwards, P. G.; Skapski, A. C.; Slawin, A. M. Z.; Wilkinson, G. *Polyhedron* **1984**, 3, 1083. (d) Beard, J. H.; Casey, J.; Murmann, R. K. *Inorg. Chem.* **1965**, 4, 797. (e) Murmann, R. K.; Schlemper, E. O. *Inorg. Chem.* **1971**, 10, 2352.

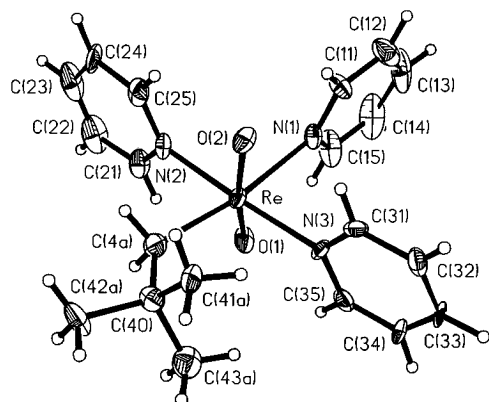


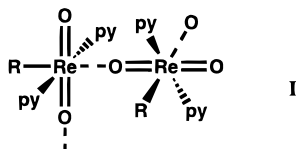
Figure 4. Plot of $\text{ReO}_2(\text{CH}_2\text{CMe}_3)(\text{py})_3$ showing the atom-numbering scheme (30% probability level ellipsoids).

127°; molecule B, 130°), but this is probably an artifact of the disorder in the neopentyl ligand.

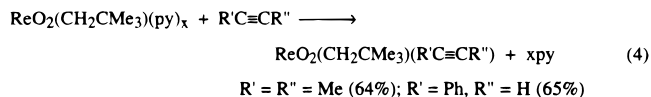
The Re–N distances to the mutually trans py ligands (N(2) and N(3), average 2.147(11) Å) are normal; for example, they are close to those observed in $[\text{ReO}_2(\text{py})_4]^+$, $[\text{ReO}_2(\text{en})_2]^+$, and $[\text{ReO}_2(4\text{-py-Me})_4]^+$.^{18a,e} The Re–N distance to the py trans to the neopentyl group (2.348(11) Å), however, is about 0.2 Å longer than the average of the other two Re–N distances due to the strong trans influence of the alkyl ligand.

Consistent with the solid-state structure, the ^1H NMR spectrum for $\text{ReO}_2(\text{CH}_2\text{CMe}_3)(\text{py})_3$ in CD_2Cl_2 at -70°C reveals two singlets in the integral ratio of 2:9 assigned to the methylene and methyl protons of the neopentyl ligand which are assigned to the *ortho*-, *meta*-, and *para*-protons of the two different types of pyridine ligands. As the solution is warmed, the two sets of multiplet resonances merge together into one set, indicating pyridine ligand exchange. The sample begins to decompose at -10°C , producing unidentified products. When a $\text{CD}_2\text{Cl}_2/\text{pyridine-}d_5$ (≈ 100 equiv) mixture is added to $\text{ReO}_2(\text{CH}_2\text{CMe}_3)(\text{py})_3$, the compound is stabilized by the excess pyridine and a room-temperature ^1H NMR spectrum can be recorded. Under these conditions, the pyridine- d_5 exchanged with all of the pyridine ligands according to the NMR spectrum.

IR spectra recorded for Nujol mulls of $\text{ReO}_2(\text{CH}_2\text{CMe}_3)(\text{py})_x$, $x \approx 2$ or 3, are nearly identical. Both show a strong band at 803 cm^{-1} that can be assigned to the antisymmetric stretch of the *trans*-dioxo group.¹² The IR spectra also show bands near 1600 cm^{-1} , which are assigned to the pyridine ligands. The similarity of the IR spectra suggests that $\text{ReO}_2(\text{CH}_2\text{CMe}_3)(\text{py})_2$ has a structure akin to $\text{ReO}_2(\text{CH}_2\text{CMe}_3)(\text{py})_3$. A possible structure is **I**.



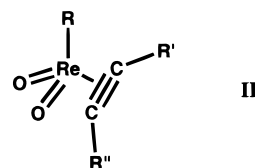
$\text{ReO}_2(\text{CH}_2\text{CMe}_3)(\text{alkyne})$. $\text{ReO}(\text{CH}_2\text{CMe}_3)(\text{py})_x$ reacts with 2-butyne in toluene/pyridine and with neat $\text{PhC}\equiv\text{CH}$ to give alkyne adducts (eq 4). Isolation of the adducts is accomplished by vacuum sublimation. The isolated phenylacetylene complex is a 5:1 mixture of two isomers.



IR spectra for the alkyne adducts show two strong bands (e.g., 966 and 921 cm^{-1} for the 2-butyne adduct) assigned to the symmetric and antisymmetric stretches of *cis*-dioxo groups. These are similar to those reported for $\text{ReO}_2(\text{Me})(\text{alkyne})$ (alkyne = 2-butyne and phenylacetylene).¹⁹ The IR spectra also show weak–medium intensity bands at 1836 cm^{-1} for $\text{ReO}_2(\text{CH}_2\text{CMe}_3)(\text{MeC}\equiv\text{CMe})$ and 1738 cm^{-1} for $\text{ReO}_2(\text{CH}_2\text{CMe}_3)(\text{PhC}\equiv\text{CH})$ that are assigned to the alkyne carbon–carbon bond stretches. These values are $\approx 400\text{ cm}^{-1}$ lower than for the free alkynes²⁰ suggesting strong back-bonding and concomitant C–C bond order reduction.

The ^1H NMR spectrum for $\text{ReO}_2(\text{CH}_2\text{CMe}_3)(\text{MeC}\equiv\text{CMe})$ has two singlets in a 2:9 ratio assigned to the methylene and methyl protons of the neopentyl ligand and two quartets ($^5J_{\text{HH}} = 1.03\text{ Hz}$) in a 1:1 ratio assigned to the methyl protons of the 2-butyne ligand. This suggests that the Re– CH_2 and $\text{C}\equiv\text{C}$ vectors lie in a mirror plane that bisects the O–Re–O angle. $^{13}\text{C}\{^1\text{H}\}$ NMR spectra for the adducts have resonances in the region 125–140 ppm assigned to the acetylenic carbons of the alkyne ligands.

On the basis of the spectroscopic data, the adducts are proposed to have tetrahedral-like structures, **II**. The proposed structure is the same as found for structurally characterized $\text{ReO}_2(\text{Me})(\text{PhC}\equiv\text{CPh})$.¹⁹



NOE NMR experiments were used to distinguish the two isomers of $\text{ReO}_2(\text{CH}_2\text{CMe}_3)(\text{PhC}\equiv\text{CH})$. The results clearly show that the neopentyl-ligand methylene protons are closer to the acetylene proton in the major isomer than in the minor isomer; thus, the major isomer is the one in which the Ph group is farther away from the neopentyl ligand (i.e., $\text{R}'' = \text{Ph}$ in **II**). This isomer is favored because it is the less sterically crowded than the other.

Discussion

We have presented the synthesis of three new 5-coordinate Re(VII) dioxo compounds of the type $\text{ReO}_2(\text{CH}_2\text{CMe}_3)_2\text{R}$ and an improved synthesis of $\text{ReO}_2(\text{CH}_2\text{CMe}_3)_3$. Prior to this work, the only reported compounds of this kind were ReO_2R_3 , $\text{R} = \text{Me}$,⁷ CH_2CMe_3 ,^{8c} and CH_2SiMe_3 ,^{8a} and related compounds such as $\text{ReO}_2(\text{CH}_2\text{CMe}_3)_2\text{X}$, $\text{X} = \text{halide}$, alkoxide, and thiolate,^{8b,e} and ReO_2MeX_2 , $\text{X}_2 = \text{chelating dialkoxide}$.^{9a–c}

It is interesting that the low-temperature-limiting ^1H NMR spectrum of $\text{ReO}_2(\text{CH}_2\text{CMe}_3)_2(\text{CH}_2\text{SiMe}_3)$ is con-

(19) Felixberger, J. K.; Kuchler, J. G.; Herdtweck, E.; Paciello, R. A.; Herrmann, W. A. *Angew. Chem., Int. Ed. Engl.* **1988**, *27*, 946. Herrmann, W. A.; Felixberger, J. K.; Kuchler, J. G.; Herdtweck, E. *Z. Naturforsch. B* **1990**, *45*, 876.

(20) Dollish, F. R.; Fateley, W. G.; Bentley, F. F. *Characteristic Raman Frequencies of Organic Compounds*; John Wiley & Sons: New York, 1974; pp 153–155.

sistent with it having the same distorted structure as ReO_2R_3 ($\text{R} = \text{CH}_2\text{CMe}_3$, CH_2SiMe_3).^{8c} $\text{ReO}_2(\text{CH}_2\text{CMe}_3)_3$ has a highly distorted tbp structure in the solid state in which the axial methylene groups lean toward one of the oxo ligands. The driving force for the distorted geometry in $\text{ReO}_2(\text{CH}_2\text{CMe}_3)_3$ was postulated to be an interaction between one of the oxo ligands and the axial methylene protons. Steric factors were specifically excluded as being the cause of the distortion. In contrast, we have found that $\text{ReO}_2(\text{CH}_2\text{CMe}_3)_2\text{Ph}$ does not have a distorted geometry in the solid state, nor does it appear to adopt a distorted geometry in solution. If the hypothesis concerning oxo–methylene interactions in ReO_2R_3 ($\text{R} = \text{CH}_2\text{CMe}_3$, CH_2SiMe_3) is correct, then it is unclear why $\text{ReO}_2(\text{CH}_2\text{CMe}_3)_2\text{Ph}$ does not show similar interactions and structural distortions. On this basis, it is possible that the distorted structures of $\text{ReO}_2\text{R}'_2\text{R}$ ($\text{R}' = \text{CH}_2\text{CMe}_3$, $\text{R} = \text{CH}_2\text{CMe}_3$ or CH_2SiMe_3 ; $\text{R}' = \text{R} = \text{CH}_2\text{SiMe}_3$) are in fact due to steric factors and the original hypothesis concerning oxo–methylene interactions is incorrect.²¹

Our results show that photolysis of $\text{ReO}_2(\text{CH}_2\text{CMe}_3)_3$ in pyridine or acetonitrile gives $\text{ReO}_2(\text{CHCMe}_3)(\text{CH}_2\text{CMe}_3)$ and neopentane by α -elimination, but photolysis or thermolysis of $\text{ReO}_2(\text{CH}_2\text{CMe}_3)_2\text{Ph}$ in pyridine gives $\text{Re(V)} \text{ReO}_2(\text{CH}_2\text{CMe}_3)(\text{py})_3$ and neopentylbenzene by (formal) reductive elimination. Although it is somewhat surprising the reduction occurs given the marked propensity of rhenium to form Re–C multiple bonds, we have previously reported that photolysis of $\text{ReO}_2(\text{CH}_2\text{SiMe}_3)_3$ also induces reduction, giving $\text{Re(VI)} [\text{Re}(\mu\text{-O})\text{O}(\text{CH}_2\text{SiMe}_3)_2]_2$.^{8a} The instability of $\text{ReO}_2(\text{CH}_2\text{CMe}_3)(\text{py})_3$ in the absence of excess pyridine, conditions which favor formation of $\text{ReO}_2(\text{CH}_2\text{CMe}_3)(\text{py})_x$ where $x < 3$, is also surprising, and the reason for the instability is not clear.

The formation of $\text{ReO}_2(\text{CHCMe}_3)(\text{CH}_2\text{CMe}_3)(\text{quin})$ from $\text{ReO}_2(\text{CHCMe}_3)(\text{CH}_2\text{CMe}_3)$ indicates that the latter is electrophilic and sterically open enough to bind a potent donor ligand. The Re–N distance is long and presumably weak, however, due to the strong trans influence of the neopentyl ligand. This may explain why $\text{ReO}_2(\text{CHCMe}_3)(\text{CH}_2\text{CMe}_3)$ does not react with weak donors such as alkynes or olefins. If 4-coordinate derivatives with ligands that have less trans influence than an alkyl could be prepared, such as $\text{ReO}_2(\text{CHCMe}_3)\text{X}$ ($\text{X} = \text{halide, alkoxide}$), they may bind alkynes or olefins thereby leading to Re=C bond reactivity.

The alkylidene and Re(V) chemistry we have described is closely related to Schrock and co-workers' imido chemistry. They showed, for example, that $\text{Re}(\text{NCMe}_3)_2(\text{CHSiMe}_3)(\text{CH}_2\text{SiMe}_3)_3$ is cleanly formed upon photolysis of $\text{Re}(\text{NCMe}_3)_2(\text{CH}_2\text{SiMe}_3)_3$, while the related imido–neopentylidene derivative apparently forms spontaneously via a $\text{Re}(\text{NCMe}_3)_2(\text{CH}_2\text{CMe}_3)_3$ intermediate. Schrock and co-workers have also synthesized $\text{Re}(\text{N-2,6-}i\text{-Pr}_2\text{C}_6\text{H}_3)_2(\text{CH}_2\text{CMe}_3)(\text{py})_2$, an imido analog of $\text{ReO}_2(\text{CH}_2\text{CMe}_3)(\text{py})_3$, by reducing $\text{Re}(\text{N-2,6-}i\text{-Pr}_2\text{C}_6\text{H}_3)_2(\text{CH}_2\text{CMe}_3)\text{Cl}_2$ or alkylating $\text{Re}(\text{N-2,6-}i\text{-Pr}_2\text{C}_6\text{H}_3)_2\text{Cl}(\text{py})_2$.²² $\text{Re}(\text{N-2,6-}i\text{-Pr}_2\text{C}_6\text{H}_3)_2(\text{CH}_2\text{CMe}_3)(\text{py})_2$ reacts with π acceptors and phosphine to form $\text{Re}(\text{N-2,6-}i\text{-Pr}_2\text{C}_6\text{H}_3)_2(\text{CH}_2\text{CMe}_3)\text{L}$

($\text{L} = \text{PMe}_2\text{Ph}$, $\eta^2\text{-2-butyne}$, $\eta^2\text{-Me}_2\text{C=O}$, $\eta^2\text{-}t\text{-Bu(H)C=O}$, $\eta^2\text{-norbornene}$), compounds that are analogous to $\text{ReO}_2(\text{CH}_2\text{CMe}_3)(\text{alkyne})$. Also pertinent is Herrmann and co-workers' phosphine reduction of MeReO_3 to produce the putative Re(V) intermediate, $\text{ReO}_2\text{Me}(\text{OPR}_3)$, which is subsequently trapped by alkyne to give $\text{ReO}_2\text{Me}(\text{alkyne})$.¹⁹

Finally, we mention in passing the large O–Re–O angles observed in $\text{ReO}_2(\text{CH}_2\text{CMe}_3)_2\text{Ph}$ ($123.8(2)^\circ$), $\text{ReO}_2(\text{CHCMe}_3)(\text{CH}_2\text{CMe}_3)$ ($124.6(4)^\circ$), and $\text{ReO}_2(\text{CHCMe}_3)(\text{CH}_2\text{CMe}_3)(\text{quin})$ ($133.3(2)^\circ$). Previously, we structurally characterized $\text{ReO}_2(\text{CH}_2\text{CMe}_3)_2\text{Br}(\text{py})$, $\text{ReO}_2(\text{CH}_2\text{CMe}_3)_3$, $[\text{ReO}_2(\text{CH}_2\text{CMe}_3)_2]_2(\mu\text{-O})$, and $\text{ReO}_2(\text{CH}_2\text{CMe}_3)_2(\text{SPh})$ having O–Re–O angles of $107.4(3)^\circ$, $117.4(5)^\circ$,^{8c} $107.5(6)^\circ$ (av),^{8e} and $117.7(3)^\circ$,^{8e} respectively. Typically, d^0 4-, 5-, and 6-coordinate transition-metal dioxo complexes have O–M–O angles in a narrow range of $105\text{--}115^\circ$, although most of the structural data comes from group 5 and 6 complexes. The wide range of angles observed for the rhenium compounds suggests they have a shallower energy potential for O–M–O variation than do the early transition metal complexes, but a firm conclusion or a rationalization for why this may be the case should be deferred until more rhenium-(VII) dioxo complexes are structurally characterized.

Conclusion

ZnR_2 alkylation of $\text{ReO}_2(\text{CH}_2\text{CMe}_3)_2\text{X}(\text{py})$ at low temperature gives $\text{ReO}_2(\text{CH}_2\text{CMe}_3)_2\text{R}$ ($\text{R} = \text{Me}$, CH_2CMe_3 , CH_2SiMe_3 , Ph) in high yield. The crystal structure of $\text{ReO}_2(\text{CH}_2\text{CMe}_3)_2\text{Ph}$ shows that it has a distorted trigonal bipyramidal structure with the oxo and Ph ligands in the equatorial plane. Photolysis of $\text{ReO}_2(\text{CH}_2\text{CMe}_3)_3$ in pyridine gives neopentane and $\text{ReO}_2(\text{CHCMe}_3)(\text{CH}_2\text{CMe}_3)$. $\text{ReO}_2(\text{CHCMe}_3)(\text{CH}_2\text{CMe}_3)$ reacts with quinuclidine to give $\text{ReO}_2(\text{CHCMe}_3)(\text{CH}_2\text{CMe}_3)(\text{quin})$, but it does not react with olefins. In the solid state, $\text{ReO}_2(\text{CHCMe}_3)(\text{CH}_2\text{CMe}_3)$ has a distorted tetrahedral structure, and $\text{ReO}_2(\text{CHCMe}_3)(\text{CH}_2\text{CMe}_3)(\text{quinuclidine})$ is trigonal bipyramidal with the neopentylidene and oxo ligands defining the equatorial plane. The long Re–N distance suggests a weak quinuclidine interaction. Thermolysis of $\text{ReO}_2(\text{CH}_2\text{CMe}_3)_2\text{Ph}$ in pyridine gives $\text{ReO}_2(\text{CH}_2\text{CMe}_3)(\text{py})_3$ and neopentylbenzene. An X-ray structure of $\text{ReO}_2(\text{CH}_2\text{CMe}_3)(\text{py})_3$ shows that it has an octahedral structure with trans oxo groups. $\text{ReO}_2(\text{CH}_2\text{CMe}_3)(\text{py})_3$ readily loses pyridine and reacts with alkynes to form $\text{ReO}_2(\text{CH}_2\text{CMe}_3)(\text{alkyne})$.

Experimental Section

All manipulations and reactions were carried out under an atmosphere of dry, oxygen-free nitrogen or argon by using standard Schlenk techniques or dryboxes. Solvents were purified by standard techniques. Proton and ^{13}C NMR spectra were referenced internally to solvent ^1H and ^{13}C resonances, respectively. Infrared spectra were referenced externally to the 1601 cm^{-1} band of polystyrene. $\text{ReO}_2(\text{CH}_2\text{CMe}_3)_2\text{X}(\text{py})$ ($\text{X} = \text{Cl}$, Br) was prepared from $[\text{Re}(\mu\text{-O})\text{O}(\text{CH}_2\text{CMe}_3)_2]_2$ as described previously.^{8b} ZnR_2 ($\text{R} = \text{Me}$, CH_2SiMe_3 , CH_2CMe_3) compounds were prepared as described in the literature.²³

(21) If this is the case, then the long Re–O distance observed^{8c} in $\text{ReO}_2(\text{CH}_2\text{CMe}_3)_3$ is probably due to a crystallography error, although we have subsequently not been able to identify any obvious problem with the data or structure refinement.

(22) Williams, D. S.; Schofield, M. H.; Schrock, R. R. *Organometallics* **1993**, *12*, 4560. Weinstock, I. A.; Schrock, R. R.; Williams, D. S.; Crowe, W. E. *Organometallics* **1991**, *10*, 1.

ZnPh₂. In a three-neck round bottom flask equipped with a condenser and a liquid-dropping funnel was placed dry ZnCl₂ (7.00 g, 51.4 mmol) and diethyl ether (250 mL). To the mixture was slowly added a light brown solution of Mg(Ph)Br in diethyl ether (3.1 M, 105 mmol) via the dropping funnel. The mixture was stirred at room temperature for 12 h and then refluxed for 3 h after the addition was completed. The mixture was cooled to room temperature and filtered, and the solids that were collected on the frit were discarded. The volatile components were removed under vacuum from the light brown filtrate, and the residue was extracted with toluene (1 × 200 mL, 1 × 20 mL). The extracts were combined, and the volume was reduced under vacuum to ≈100 mL. Cooling the solution to -50 °C produced colorless crystals which were isolated by removing the mother liquor via a cannula. The crystals were dried under vacuum (yield 6.07 g, 54%). ¹H NMR (CD₃CN): δ 7.62 (m, 2, Ph), 7.13 (m, 3, Ph).

ReO₂(CH₂CMe₃)₃. ReO₂(CH₂CMe₃)₂Cl(py) was produced in situ by reacting ReO₂(CH₂CMe₃)₂Br(py) (0.199 g, 0.38 mmol) with AgCl (0.110 g, 0.76 mmol) in CH₂Cl₂ (20 mL). The mixture was stirred at 23 °C for 12 h. The solvent was then removed in vacuo, and the residue was extracted with toluene (1 × 10 mL, 2 × 5 mL). The red extracts, containing ReO₂(CH₂CMe₃)₂Cl(py), were combined and cooled to -5 °C. A colorless solution of Zn(CH₂CMe₃)₂ (0.160 g, 0.77 mmol) in toluene (5 mL) was then very slowly added to the cold solution via a liquid-dropping funnel. After the addition was completed, the reaction mixture was stirred at -5 °C for 30 min and then warmed to room temperature. The mixture was then stripped in vacuo. Sublimation from the residue in vacuo (45 °C, 10⁻³ mmHg) gave an orange powder on an H₂O-cooled cold finger (yield 0.130 g, 79%). Spectroscopic data was published previously.^{8c}

ReO₂(CH₂CMe₃)₂Me. ReO₂(CH₂CMe₃)₂Cl(py) (0.180 g, 0.38 mmol) was dissolved in toluene (20 mL), and the red solution was cooled to -40 °C. ZnMe₂ (0.036 g, 0.38 mmol) in toluene (5 mL) was slowly added to the cold solution via a liquid-dropping funnel. A white solid formed during the addition. After the addition was completed, the mixture was warmed to room temperature and then filtered. The filtrate was carefully stripped, leaving an oily residue. The oil was further dried under vacuum at 0 °C for 5 h. Sublimation/distillation from the oil in vacuo (23 °C, 10⁻³ mmHg) gave an orange solid on a CO₂-cooled cold finger (yield 0.122 g, 86%). The solid melts near room temperature. Anal. Calcd for C₁₁H₂₅O₂Re: C, 35.18; H, 6.71. Found: C, 35.04; H, 6.68.

¹H NMR (C₆D₆): δ 3.05 (s, 4, CH₂CMe₃), 1.51 (s, 3, Me), 1.07 (s, 18, CH₂CMe₃). ¹³C{¹H} NMR (C₆D₆): δ 71.4 (s, 2, CH₂CMe₃), 35.5 (s, 2, CH₂CMe₃), 33.2 (s, 1, Me), 31.63 (s, 6, CH₂CMe₃). IR (neat, CsI, cm⁻¹): ν(Re=O) 992 s and 946 s.

ReO₂(CH₂CMe₃)₂(CH₂SiMe₃). ReO₂(CH₂CMe₃)₂Br(py) (0.130 g, 0.25 mmol) was dissolved in toluene (20 mL), and the resulting red solution was cooled to 0 °C. Zn(CH₂SiMe₃)₂ (0.084 g, 0.35 mmol) in toluene (5 mL) was slowly added to the cold solution via a liquid-dropping funnel. After the addition was completed, the mixture was stirred at 0 °C for 30 min, warmed to room temperature, and then stirred for another 30 min. Oxygen-free water (0.5 mL) was then added to the mixture, giving a cloudy solution. The cloudy solution was cooled to -20 °C to freeze the excess water and then cold filtered. The filtrate was stripped under vacuum. Sublimation from the residue (23 °C, 10⁻³ mmHg) gave an orange solid on an H₂O-cooled cold finger (yield 0.095 g, 85%). Anal. Calcd for C₁₄H₃₃SiO₂Re: C, 37.56; H, 7.43. Found: C, 37.43; H, 7.28.

¹H NMR (CD₂Cl₂, 23 °C): δ 3.25 (s, 4, CH₂CMe₃), 1.84 (s, 2, CH₂SiMe₃), 1.08 (s, 18, CH₂CMe₃), 0.17 (s, 9, CH₂SiMe₃). ¹H NMR (CD₂Cl₂, -86 °C): δ 3.20 and 3.13 (AB q, 4, J_{HH} = 13.8

Hz, CH₂CMe₃), 1.81 (s, 2, CH₂SiMe₃), 0.96 (s, 18, CH₂CMe₃), 0.05 (s, 9, CH₂SiMe₃). ¹³C{¹H} NMR (CD₂Cl₂, 23 °C): δ 72.7 (s, 2, CH₂CMe₃), 45.1 (s, 1, CH₂SiMe₃), 35.9 (s, 2, CH₂CMe₃), 31.8 (s, 6, CH₂CMe₃), 1.89 (s, 3, CH₂SiMe₃). ¹³C{¹H} NMR (CD₂Cl₂, -86 °C): δ 72.0 (s, 2, CH₂CMe₃), 44.6 (s, 1, CH₂SiMe₃), 34.9 (s, 2, CH₂CMe₃), 30.6 (s, 6, CH₂CMe₃), 0.43 (s, 3, CH₂SiMe₃). IR (Nujol, CsI, cm⁻¹): ν(Re=O) 992 s and 945 s.

ReO₂(CH₂CMe₃)₂Ph. ReO₂(CH₂CMe₃)₂Br(py) (0.200 g, 0.38 mmol) was dissolved in toluene (20 mL), and the resulting red solution was cooled to 0 °C. ZnPh₂ (0.085 g, 0.38 mmol) in toluene (15 mL) was slowly added to the cold solution via a liquid-dropping funnel. After the addition was completed, the mixture was warmed to room temperature and then stirred for 30 min. Oxygen-free water (0.2 mL) was added to the mixture, producing a cloudy solution. The mixture was cooled to -20 °C to freeze the excess water and then cold filtered. The filtrate was stripped under vacuum. Sublimation from the residue (23 °C, 10⁻³ mmHg) gave an orange solid on an H₂O-cooled cold finger (yield 0.155 g, 92%). Anal. Calcd for C₁₆H₂₇O₂Re: C, 43.92; H, 6.22. Found: C, 43.94; H, 6.27.

¹H NMR (CD₃CN): δ 7.30 (m, 2, Ph (meta)), 7.05 (m, 2, Ph (ortho)), 6.97 (m, 1, Ph (para)), 3.42 (s, 4, CH₂CMe₃), 1.07 (s, 18, CH₂CMe₃). ¹³C{¹H} NMR (CDCl₃): δ 131.0 (s, 2, Ph (meta)), 130.5 (s, 2, Ph (ortho)), 124.1 (s, 1, Ph (para)), 75.9 (s, 2, CH₂CMe₃), 36.4 (s, 2, CH₂CMe₃), 31.8 (s, 6, CH₂CMe₃). IR (Nujol, CsI, cm⁻¹): ν(Re=O) 987 s and 945 s.

ReO₂(CHCMe₃)(CH₂CMe₃). ReO₂(CH₂CMe₃)₃ (0.179 g, 0.41 mmol) was dissolved in pyridine (20 mL). The orange solution was photolyzed with a medium-pressure mercury lamp at 23 °C for 1.5 h. The color gradually changed to deep red. The volatile components were removed under vacuum. A yellow solid sublimed from the residue (40 °C, 10⁻³ mmHg) onto a dry ice-cooled cold finger (yield 0.114 g, 76%). Anal. Calcd for C₁₀H₂₁O₂Re: C, 33.41; H, 5.89. Found: C, 33.40; H, 5.87.

¹H NMR (C₇D₈): δ 12.07 (s, 1, CHCMe₃), 2.86 and 2.63 (d of an AB q, 2, J_{HH} = 14.3 Hz, CH₂CMe₃), 0.96 (s, 9, CHCMe₃), 0.95 (s, 9, CH₂CMe₃). ¹³C NMR (C₇D₈): δ 283.3 (d, 1, J_{CH} = 138 Hz, CHCMe₃), 45.3 (s, 1, CHCMe₃), 38.5 (t, 1, J_{CH} = 130 Hz, CH₂CMe₃), 32.1 (q, 3, J_{CH} = 127 Hz, CHCMe₃), 31.3 (s, 1, CH₂CMe₃), 29.9 (q, 3, J_{CH} = 127 Hz, CH₂CMe₃). IR (Nujol, CsI, cm⁻¹): ν(Re=O) 986 s and 947 s.

ReO₂(CHCMe₃)(CH₂CMe₃)(quin). ReO₂(CH₂CMe₃)₃ (0.413 g, 0.96 mmol) was dissolved in pyridine (20 mL). The orange solution was photolyzed with a medium-pressure mercury lamp at 23 °C for 1 h. The color gradually changed to deep red. Quinuclidine (0.106 g, 0.96 mmol) was added to the red solution, and the mixture was stirred for 2 h. The volatile components were then removed in vacuo from the mixture, and the residue was redissolved in a minimum amount of acetonitrile. Slow cooling of the acetonitrile solution to -40 °C gave yellow needles, which were isolated by decanting the mother liquor via a cannula. The crystals were washed with a small amount of cold (-40 °C) acetonitrile and dried under vacuum (yield 0.244 g, 54%). A satisfactory carbon analysis was not obtained. Anal. Calcd for C₁₇H₃₄NO₂Re: C, 43.38; H, 7.28; N, 2.98. Found: C, 44.17; H, 7.33; N, 2.87.

¹H NMR (C₆D₆): δ 12.64 (s, 1, CHCMe₃), 2.51 and 2.24 (d of an AB q, 2, J_{HH} = 13.7 Hz, CH₂CMe₃), 1.25 (s, 9, CHCMe₃), 1.05 (s, 9, CH₂CMe₃), 2.65 (m, 6, quin (α)), 1.34 (m, 1, quin (γ)), 1.11 (m, 6, quin (β)). ¹³C NMR (C₆D₆): δ 291 (d, J_{CH} = 137 Hz, CHCMe₃), 49.0 (t, 3, J_{CH} = 140 Hz, quin (α)), 45.1 (s, 1, CHCMe₃), 42.9 (t, 1, J_{CH} = 128 Hz, CH₂CMe₃), 32.9 (q, 3, J_{CH} = 126 Hz, CHCMe₃), 29.9 (q, 3, J_{CH} = 127 Hz, CH₂CMe₃), 26.6 (t, 3, J_{CH} = 128 Hz, quin (β)), 21.3 (d, 1, J_{CH} = 135 Hz, quin (γ)). IR (CsI, Nujol, cm⁻¹): ν(Re=O) 946 s and 903 s.

ReO₂(CH₂CMe₃)(py)₂. ReO₂(CH₂CMe₃)₂Ph (0.410 g, 0.94 mmol) was dissolved in pyridine (20 mL). The orange solution was heated at 70 °C for 2 h in the dark. The color gradually changed to deep red. The reaction mixture was reduced in volume in vacuo (to ≈3 mL) and then cooled to -20 °C. This produced red crystals which were isolated by removing the

(23) ZnMe₂ was prepared according to the method described in: Wierda, D. A. Ph.D. Dissertation, Harvard University, 1990. Schrock, R. R.; Fellman, J. D. *J. Am. Chem. Soc.* **1978**, *100*, 3359. Moorehouse, S.; Wilkinson, G. *J. Chem. Soc.* **1974**, 2187.

Table 5. Crystal Data Summary for $\text{ReO}_2(\text{CH}_2\text{CMe}_3)_2\text{Ph}$, $\text{ReO}_2(\text{CH}_2\text{CMe}_3)(\text{py})_3$, $\text{ReO}_2(\text{CHCMe}_3)(\text{CH}_2\text{CMe}_3)$, and $\text{ReO}_2(\text{CHCMe}_3)(\text{CH}_2\text{CMe}_3)(\text{quin})$

	$\text{ReO}_2(\text{CH}_2\text{CMe}_3)_2\text{Ph}$	$\text{ReO}_2(\text{CHCMe}_3)(\text{CH}_2\text{CMe}_3)$	$\text{ReO}_2(\text{CHCMe}_3)(\text{CH}_2\text{CMe}_3)(\text{quin})$	$\text{ReO}_2(\text{CH}_2\text{CMe}_3)(\text{py})_3$
diffractometer	Nicolet R3m/V	Nicolet R3m/V	Nicolet R3m/V	Nicolet R3m/V
radiation type	Mo $K\alpha$ (monochromated)	Mo $K\alpha$ (monochromated)	Mo $K\alpha$ (monochromated)	Mo $K\alpha$ (monochromated)
wavelength, Å	0.710 73	0.710 73	0.710 73	0.710 73
color of cryst/habit	yellow-orange blocks	yellow needles	yellow blocks	red plates
empirical formula	$\text{C}_{16}\text{H}_{27}\text{O}_2\text{Re}$	$\text{C}_{10}\text{H}_{21}\text{O}_2\text{Re}$	$\text{C}_{17}\text{H}_{34}\text{NO}_2\text{Re}$	$\text{C}_{20}\text{H}_{26}\text{N}_3\text{O}_2\text{Re}$
cryst dimens, mm	$0.34 \times 0.60 \times 0.62$	$0.15 \times 0.20 \times 0.25$	$0.20 \times 0.22 \times 0.25$	$0.10 \times 0.13 \times 0.19$
space group	$P2_1/c$	Pbca	$P1$	$P2_1/n$
temp, °C	−50(1)	−80(1)	−80(1)	−50(1)
cell dimens				
<i>a</i> , Å	10.244(3)	11.038(2)	6.1657(15)	9.708(2)
<i>b</i> , Å	11.004(2)	20.168(4)	10.036(2)	18.670(3)
<i>c</i> , Å	15.861(4)	11.290(2)	16.012(4)	11.319(1)
α , deg			79.35(2)	
β , deg	107.17(2)		82.23(2)	95.39(1)
γ , deg			89.29(2)	
<i>Z</i> (molecules/cell)	4	8	2	4
<i>V</i> , Å ³	1708	2513	965	2042
<i>d</i> _{calcd} , g cm ^{−3}	1.70	1.90	1.62	1.71
abs coeff, cm ^{−1}	72.06	97.76	63.87	60.47
scan type	$\theta-2\theta$	$\theta-2\theta$	$\theta-2\theta$	$\theta-2\theta$
2θ range, deg	4–50	4–50	4–50	4–50
data collcd	$\pm h, -k, l$	$h, -k, l$ (+Friedel)	$h, \pm k, \pm l$	$-h, \pm k, \pm l$
reflens collcd	3334	3678	3766	4207
no. of unique reflens	3015	1646	3403	2688
no. with $F_o > n\sigma(F_o)$	2499 ($n = 6$)	1369 ($n = 4$)	3264 ($n = 6$)	1956 ($n = 4$)
R_{merg}^a	0.0301	0.0313	0.0279	0.0446
$R(F)^b$	0.0385	0.0384	0.0317	0.0482
$R_w(F)^c$	0.0502	0.0394	0.0416	0.0542
"goodness of fit" ^d	0.85	1.38	2.28	1.13

^a $R_{\text{merg}} = [(\sum N \sum w(F_o(\text{mean}) - F_o)^2) / (\sum (N - 1) \sum w F_o^2)]^{1/2}$, where the inner summations are over the *N* equivalent reflections averaged to give $F(\text{mean})$ and the outer summations are over all unique observed reflections. ^b $R = \sum ||F_o| - |F_c|| / \sum |F_o|$. ^c $R_w = [\sum w(|F_o| - |F_c|)^2 / \sum w |F_o|^2]^{1/2}$, $w = [\sigma^2(F) + gF^2]^{-1}$. ^d GOF = $[\sum w(|F_o| - |F_c|)^2 / (n_{\text{obs}} - n_{\text{params}})]^{1/2}$.

mother liquor via a cannula. Drying the crystals at 23 °C in vacuo for 12 h gave a value of 1.9 for *x* (on this basis, the yield is 74%). The sample prepared for combustion analysis was recrystallized from pyridine at −20 °C and then dried under vacuum at −20 °C for 2 h. A stoichiometry of $\text{ReO}_2(\text{CH}_2\text{CMe}_3)(\text{py})_{2.8}$ was calculated for this sample by using ¹H NMR. Anal. Calcd for $\text{C}_{20}\text{H}_{26}\text{N}_3\text{O}_2\text{Re}$: C, 45.61; H, 4.98; N, 7.98. Found: C, 43.73; H, 4.40; N, 7.59.

¹H NMR (CD_2Cl_2 , −70 °C): δ 9.05 (m, 2, py (ortho)), 8.76 (m, 4, py (ortho)), 7.56 (m, 1, py (para)), 7.42 (m, 2, py (para)), 7.27 (m, 2, py (meta)), 7.27 (m, 4, py (para)). ¹³C{¹H} NMR (CD_2Cl_2 , −70 °C): δ 149.4 (s, 4, py (ortho)), 146.3 (s, 2, py (meta)), 137.6 (s, 1, py (para)), 137.5 (s, 2, py (para)), 123.4 (s, 4, py (meta)), 123.3 (s, 2, py (meta)), 37.7 (s, 1, CH_2CMe_3), 35.4 (s, 1, CH_2CMe_3), 31.7 (s, 3, CH_2CMe_3). IR (Nujol, CsI, cm^{−1}): $\nu(\text{Re}=\text{O})$ 803 s.

$\text{ReO}_2(\text{CH}_2\text{CMe}_3)(\text{MeC}\equiv\text{CMe})$. $\text{ReO}_2(\text{CH}_2\text{CMe}_3)(\text{py})_{1.9}$ (0.113 g, 0.26 mmol) was dissolved in a mixture of pyridine (0.2 mL) and toluene (10 mL). The red solution was frozen in liquid nitrogen. 2-Butyne (1.5 mmol) was then condensed into the reaction flask via a calibrated vacuum manifold. The mixture was slowly warmed to room temperature and then stirred for 8 h. The color changed to light brown. The mixture was then stripped in vacuo. Sublimation from the residue in vacuo (50 °C, 10^{−3} mmHg) gave a yellow solid on an H₂O-cooled cold finger (yield 0.056 g, 64%). Anal. Calcd for $\text{C}_9\text{H}_{17}\text{O}_2\text{Re}$: C, 31.48; H, 4.99. Found: C, 31.78; H, 5.07.

¹H NMR (CDCl_3): δ 3.47 (s, 2, CH_2CMe_3), 2.89 (q, 3, ⁵*J*_{HH} = 1.03 Hz, $\text{MeC}\equiv\text{CMe}$), 2.58 (q, 3, ⁵*J*_{HH} = 1.03 Hz, $\text{MeC}\equiv\text{CMe}$), 1.15 (s, 9, CH_2CMe_3). ¹³C{¹H} NMR (CDCl_3): δ 138.8 (s, 1, $\text{MeC}\equiv\text{CMe}$), 130.7 (s, 1, $\text{MeC}\equiv\text{CMe}$), 48.5 (s, 1, CH_2CMe_3), 31.9 (s, 1, CH_2CMe_3), 31.6 (s, 3, CH_2CMe_3), 14.6 (s, 1, $\text{MeC}\equiv\text{CMe}$), 6.96 (s, 1, $\text{MeC}\equiv\text{CMe}$). IR (Nujol, CsI, cm^{−1}): $\nu(\text{Re}=\text{O})$ 966 s and 921 s, $\nu(\text{C}\equiv\text{C})$ 1836 w.

$\text{ReO}_2(\text{CH}_2\text{CMe}_3)(\text{HC}\equiv\text{CPh})$. $\text{ReO}_2(\text{CH}_2\text{CMe}_3)(\text{py})_{1.9}$ (0.114 g, 0.26 mmol) was dissolved in phenyl acetylene (0.2 mL). The reaction mixture was stirred at 23 °C for 8 h and then stripped under vacuum. Sublimation from the light brown residue in

vacuo (70 °C, 10^{−3} mmHg) produced a yellow solid on an H₂O-cooled cold finger (0.066 g, 65%). An unsatisfactory carbon analysis was obtained in two attempts. Anal. Calcd for $\text{C}_{13}\text{H}_{17}\text{O}_2\text{Re}$: C, 39.89; H, 4.38. Found: C, 41.94 and 41.38; H, 4.62 and 4.57.

Two isomers, in the ratio of 5:1, are present in solution. ¹H NMR (major isomer, CDCl_3): δ 9.10 (s, 1, $\text{HC}\equiv\text{CPh}$), 7.82–7.53 (m, 5, Ph), 3.85 (s, 2, CH_2CMe_3), 1.19 (s, 9, CH_2CMe_3). ¹H NMR (minor isomer, CDCl_3): δ 9.66 (s, 1, $\text{HC}\equiv\text{CPh}$), 7.53–7.39 (m, 5, Ph), 3.68 (s, 2, CH_2CMe_3), 1.12 (s, 9, CH_2CMe_3). ¹³C NMR (major product, CDCl_3): δ 140.1 (m, 1, $\text{HC}\equiv\text{CPh}$), 133.6 (d, 1, *J*_{CH} = 223 Hz, $\text{HC}\equiv\text{CPh}$), 133.1 (d of t, 2, *J*_{CH} = 163 Hz, ²*J*_{CH} = 6.5 Hz, Ph (meta)), 131.8 (d of t, 1, *J*_{CH} = 162 Hz, ²*J*_{CH} = 7.5 Hz, Ph (para)), 129.1 (d of d, 2, *J*_{CH} = 154 Hz, ²*J*_{CH} = 6.9 Hz, Ph (ortho)), 126.9 (t, 1, ²*J*_{CH} = 7.5 Hz, Ph (ipso)), 49.7 (t, 1, *J*_{CH} = 133 Hz, CH_2CMe_3), 32.3 (s, 1, CH_2CMe_3), 31.7 (q, 3, *J*_{CH} = 124 Hz, CH_2CMe_3). ¹³C NMR (minor product, CDCl_3): δ 130.1 (d of t, 1, *J*_{CH} = 163 Hz, ²*J*_{CH} = 6.9 Hz, Ph (para)), 129.7 (d of t, 2, *J*_{CH} = 162 Hz, ²*J*_{CH} = 6.85 Hz, Ph (meta)), 128.8 (d of d, 2, *J*_{CH} = 155 Hz, ²*J*_{CH} = 7.55 Hz, Ph (ortho)), 123.8 (d, 1, *J*_{CH} = 223 Hz, $\text{HC}\equiv\text{CPh}$), 50.6 (t, 1, CH_2CMe_3), 32.5 (s, 1, CH_2CMe_3), 31.5 (q, 3, CH_2CMe_3). IR (Nujol, CsI, cm^{−1}): $\nu(\text{Re}=\text{O})$ 971 s and 933 s, $\nu(\text{C}\equiv\text{C})$ 1738 m.

X-ray Crystallography. X-ray data were collected on a Nicolet R3m/V four-circle diffractometer equipped with a LT-1 low-temperature device. Data collection was controlled using the Nicolet P3 program. Unit cell symmetry was checked with the program XCELL. Raw diffractometer data was processed with the program XDISK. The structures were solved by use of the SHELXTL-PLUS package of programs. Drawings were produced using the Nicolet program XP.

In each case, the crystal was attached to a 0.30 mm glass fiber with a minimum amount of silicon grease. The crystal was frozen in place by immersing it in a cold nitrogen stream from the low-temperature attachment. A crystal data summary is presented in Table 5.

$\text{ReO}_2(\text{CH}_2\text{CMe}_3)_2\text{Ph}$. The crystals for study were grown by low temperature crystallization from a saturated acetoni-

Table 6. Atomic Coordinates ($\times 10^5$) and Equivalent Isotropic Displacement Parameters ($\text{\AA}^2 \times 10^4$) for $\text{ReO}_2(\text{CH}_2\text{CMe}_3)_2\text{Ph}^a$

atom	x	y	z	U(eq)
Re	72189(3)	1973(2)	31409(2)	186(1)
O(1)	82825(49)	12031(50)	28507(32)	330(18)
O(2)	77528(57)	-8362(49)	39714(30)	359(19)
C(1)	62426(70)	14412(64)	38223(41)	230(22)
C(10)	71597(76)	18211(65)	47585(43)	263(24)
C(11)	71923(98)	8192(85)	54191(46)	439(32)
C(12)	86069(74)	21838(76)	47985(44)	301(25)
C(13)	64269(89)	29419(76)	49952(51)	383(30)
C(2)	69046(66)	-10834(64)	20743(40)	201(21)
C(20)	82529(76)	-15438(67)	19030(44)	261(24)
C(21)	93609(71)	-18427(75)	27380(46)	304(25)
C(22)	87407(87)	-6270(79)	13541(51)	372(28)
C(23)	78332(82)	-27213(68)	13501(49)	309(26)
C(3)	50971(70)	2763(52)	24100(44)	164(20)
C(4)	46503(77)	11551(66)	17423(41)	270(23)
C(5)	32859(82)	12274(70)	12537(43)	319(26)
C(6)	23390(83)	4374(71)	14347(51)	332(27)
C(7)	27636(78)	-4092(80)	20848(51)	313(27)
C(8)	41412(72)	-5072(68)	25725(44)	250(23)

^a Equivalent isotropic U defined as one-third of the trace of the orthogonalized U_{ij} tensor.

Table 7. Atomic Coordinates ($\times 10^4$) and Equivalent Isotropic Displacement Parameters ($\text{\AA}^2 \times 10^3$) for $\text{ReO}_2(\text{CHCMe}_3)(\text{CH}_2\text{CMe}_3)^a$

atom	x	y	z	U(eq)
Re	1523(1)	6151(1)	8220(1)	24(1)
O(2)	225(7)	6483(3)	8765(7)	38(3)
O(1)	2645(7)	5812(3)	9065(6)	37(3)
C(2)	949(9)	5409(5)	7023(8)	22(3)
C(1)	2212(9)	6690(4)	7055(8)	20(3)
C(20)	405(10)	4762(4)	7559(10)	26(3)
C(10)	1790(9)	7234(4)	6246(10)	26(3)
C(13)	465(14)	7396(8)	6398(15)	55(5)
C(11)	2016(16)	6999(6)	4973(10)	46(5)
C(22)	1378(11)	4384(6)	8269(11)	35(4)
C(21)	-678(10)	4924(5)	8363(9)	30(4)
C(23)	-26(13)	4340(6)	6528(12)	37(5)
C(12)	2566(17)	7857(6)	6490(12)	49(5)

^a Equivalent isotropic U defined as one-third of the trace of the orthogonalized U_{ij} tensor.

trile solution (-20°C ; 2 days). Removal of the mother liquor via a cannula yielded yellow-orange blocks. The crystals were handled in air for the short time necessary for selection and mounting. Atomic coordinates are given in Table 6. The intensities of three check reflections were measured after every 60 reflections. A linear decay correction based on a decay of 29% during the 40 h of data collection was applied to the data. An absorption correction using the program XEMP, which was based on ψ scans from 5 reflections near $\chi = 90^\circ$, and Lorentz and polarization corrections were applied to the data.

Systematic absences uniquely determined the space group to be $P2_1/c$. A Patterson synthesis readily revealed the position of the rhenium atom. Standard difference map techniques were used to find the remaining non-hydrogen atoms. The hydrogen atoms were placed on the carbon atoms in calculated positions [$U_{\text{iso}}(\text{H}) = 1.2U_{\text{iso}}(\text{C})$; $d_{\text{C-H}} = 0.96 \text{ \AA}$] for refinement. Refinement was performed to convergence with this model. The final difference map contained eight peaks of height greater than 1.0 e \AA^{-3} located within 1.04 \AA of the rhenium [$1.99 \text{ e \AA}^{-3} (\text{max})$].

$\text{ReO}_2(\text{CHCMe}_3)(\text{CH}_2\text{CMe}_3)$. The crystals for study were grown by slowly cooling a saturated acetonitrile solution (-20°C ; 24 h). Removal of the mother liquor via a cannula yielded yellow needles. The crystals were handled for short periods of time in air. Atomic coordinates are presented in Table 7. The intensities of three check reflections were measured after every 60 reflections; the crystal did not decay significantly during the 78 h of data collection. An absorption correction

Table 8. Atomic Coordinates ($\times 10^4$) and Equivalent Isotropic Displacement Parameters ($\text{\AA}^2 \times 10^3$) for $\text{ReO}_2(\text{CHCMe}_3)(\text{CH}_2\text{CMe}_3)(\text{quin})^a$

atom	x	y	z	U(eq)
Re	2424(1)	-832(1)	2371(1)	20(1)
O(1)	3719(7)	387(4)	1568(3)	28(1)
O(2)	-210(6)	-1474(4)	2598(3)	27(1)
C(1)	4488(10)	-1952(6)	2928(4)	25(2)
C(10)	4429(10)	-3160(6)	3633(4)	27(2)
C(11)	5412(17)	-2656(12)	4360(6)	42(3)
C(12)	5913(12)	-4253(7)	3327(5)	39(2)
C(13)	2136(10)	-3732(7)	3945(4)	30(2)
C(2)	1982(11)	433(6)	3321(4)	27(2)
C(20)	490(11)	1678(6)	3212(4)	30(2)
C(21)	-1832(15)	1299(10)	3129(9)	82(5)
C(22)	1384(20)	2741(8)	2449(6)	73(4)
C(23)	469(21)	2328(10)	4008(6)	61(4)
N	2553(8)	-2059(5)	1195(3)	22(1)
C(31)	1234(10)	-1291(6)	553(4)	28(2)
C(32)	1477(12)	-1882(7)	-278(4)	31(2)
C(33)	2579(11)	-3274(6)	-108(4)	31(2)
C(34)	1270(12)	-4095(6)	699(4)	33(2)
C(35)	1567(11)	-3457(6)	1468(4)	29(2)
C(36)	4913(11)	-3045(7)	68(4)	31(2)
C(37)	4816(10)	-2169(7)	769(4)	26(2)

^a Equivalent isotropic U defined as one-third of the trace of the orthogonalized U_{ij} tensor.

(PSICOR) based on ψ scans from 6 reflections near $\chi = 90^\circ$ and Lorentz and polarization corrections were applied to the data.

Systematic absences uniquely determined the space group to be $Pbca$. A Patterson synthesis readily revealed the position of the Re atom. Standard difference map techniques were used to find the remaining non-hydrogen atoms. After all of the non-hydrogen atoms were located and refined anisotropically, a difference map revealed all of the hydrogen atom positions. An attempt was made to refine the hydrogen atoms isotropically, but during the refinement one hydrogen attached to each of C(2) and C(21) did not refine well. Therefore, all of the hydrogen atoms attached to these two carbon atoms were placed in calculated positions [$U_{\text{iso}}(\text{H}) = 1.2U_{\text{iso}}(\text{C})$; $d_{\text{C-H}} = 0.96 \text{ \AA}$] for refinement. Refinement was performed to convergence with this model. The final difference map contained six peaks of height greater than 1.0 e \AA^{-3} located within 1.23 \AA of the rhenium [$1.56 \text{ e \AA}^{-3} (\text{max})$]. All other peaks were less than 0.69 e \AA^{-3} .

$\text{ReO}_2(\text{CHCMe}_3)(\text{CH}_2\text{CMe}_3)(\text{quin})$. The crystals for study were grown by slowly cooling a saturated acetonitrile solution (-20°C ; 12 h). Removal of the mother liquor via a cannula yielded yellow blocks. The crystals were handled for short periods of time in air. Atomic coordinates are presented in Table 8. The intensities of three check reflections were measured after every 60 reflections; the crystal did not decay significantly during the 45 h of data collection. A semiempirical absorption correction (PSICOR) based on scans from 8 reflections near $\chi = 90^\circ$ and Lorentz and polarization corrections were applied to the data.

A Patterson synthesis readily revealed the position of the Re atom. Standard difference map techniques were used to find the remaining non-hydrogen atoms. After all of the non-hydrogen atoms were located and refined anisotropically, a difference map revealed all of the hydrogen atom positions. An attempt was made to refine the hydrogen atoms isotropically, but during the refinement one hydrogen attached to each of C(21), C(22), and C(35) did not refine well. Therefore, all of the hydrogen atoms attached to these carbon atoms were placed in calculated positions [$U_{\text{iso}}(\text{H}) = 1.2U_{\text{iso}}(\text{C})$; $d_{\text{C-H}} = 0.96 \text{ \AA}$] for refinement. Refinement was performed to convergence with this model. The final difference map contained one peak of height 1.97 e \AA^{-3} located 0.88 \AA from the rhenium. All other peaks were less than 1.0 e \AA^{-3} .

$\text{ReO}_2(\text{CH}_2\text{CMe}_3)(\text{py})_3$. The crystals for study were grown by slowly cooling a saturated pyridine solution (-20°C ; 2

Table 9. Atomic Coordinates ($\times 10^4$) and Equivalent Isotropic Displacement Parameters ($\text{\AA}^2 \times 10^3$) for $\text{ReO}_2(\text{CH}_2\text{CMe}_3)(\text{py})_3$ ^a

atom	x	y	z	U(eq)
Re	797(1)	3196(1)	2747(1)	30(1)
O(1)	820(10)	3439(6)	4240(8)	52(4)
O(2)	590(9)	3160(5)	1203(8)	42(3)
N(1)	-327(11)	4304(6)	2451(11)	37(4)
N(2)	2793(11)	3668(6)	2690(11)	38(4)
N(3)	-1273(11)	2782(6)	2791(10)	33(4)
C(11)	-815(15)	4507(9)	1359(15)	54(6)
C(12)	-1545(19)	5133(10)	1151(20)	72(8)
C(13)	-1767(19)	5573(11)	2097(30)	98(11)
C(14)	-1226(21)	5363(11)	3144(23)	91(10)
C(15)	-525(17)	4739(9)	3319(17)	64(7)
C(21)	3569(16)	3870(8)	3662(16)	52(6)
C(22)	4868(21)	4158(11)	3654(24)	80(9)
C(23)	5379(21)	4257(10)	2571(31)	92(12)
C(24)	4609(18)	4078(10)	1579(23)	79(9)
C(25)	3354(16)	3768(8)	1651(16)	47(6)
C(31)	-2062(14)	2647(8)	1803(14)	43(6)
C(32)	-3437(15)	2418(8)	1823(18)	53(7)
C(33)	-4008(15)	2365(9)	2886(19)	60(7)
C(34)	-3162(15)	2511(9)	3894(17)	55(7)
C(35)	-1847(16)	2721(9)	3853(15)	50(6)
C(4A) ^b	2020(17)	2221(7)	2816(21)	54(11)
C(4B) ^c	1567(35)	2163(9)	3437(22)	67(21)
C(40)	1568(11)	1459(5)	2773(10)	42(6)
C(41A) ^b	581(18)	1307(11)	1681(16)	50(10)
C(41B) ^c	2432(31)	1556(20)	1717(23)	79(23)
C(42A) ^b	2784(18)	952(9)	2801(20)	62(12)
C(42B) ^c	122(19)	1250(18)	2311(30)	59(21)
C(43A) ^b	780(21)	1293(12)	3861(16)	64(11)
C(43B) ^c	2226(39)	881(11)	3569(23)	97(33)

^a Equivalent isotropic U defined as one-third of the trace of the orthogonalized U_{ij} tensor. ^b Site occupancy factor (SOF) associated with the disordered neopentyl group, SOF = 0.66. ^c SOF = 0.34.

days). Removal of the supernatant solution via a cannula yielded red plates. The crystals were handled under a nitrogen atmosphere. Atomic coordinates are presented in Table 9. The

intensities of three check reflections were measured after every 60 reflections. A linear decay correction based on a decay of 19% during the 63 h of data collection was applied to the data. An absorption correction using the program XEMP, which was based on scans from 6 reflections near $\chi = 90^\circ$, and Lorentz and polarization corrections were applied to the data.

Systematic absences uniquely determined the space group to be $P2_1/n$. A Patterson synthesis readily revealed the position of the rhenium atom. Standard difference map techniques were used to find the remaining non-hydrogen atoms. The neopentyl group was found to be disordered over two positions with refinement indicating a 66/34 distribution. The hydrogen atoms were placed on the carbon atoms in calculated positions [$U_{\text{iso}}(\text{H}) = 1.2U_{\text{iso}}(\text{C})$; $d_{\text{C-H}} = 0.96 \text{ \AA}$] for refinement. Refinement was performed to convergence with this model. The final difference map contained two peaks of height greater than 1.0 e \AA^{-3} located within 1.16 \AA of Re (1.34 e \AA^{-3} (max)).

Acknowledgment for support is made to the Petroleum Research Fund, administered by the American Chemical Society. D.M.H. also wishes to acknowledge support from the Robert A. Welch Foundation and the Alfred P. Sloan Foundation (1992–1994) in the final stages of this research.

Supporting Information Available: Tables of anisotropic thermal parameters, calculated H atom coordinates, and bond lengths and bond angles, a stick drawing of $\text{ReO}_2(\text{CH}_2\text{CMe}_3)(\text{py})_3$ showing the disordered neopentyl ligand, and packing diagrams for $\text{ReO}_2(\text{CH}_2\text{CMe}_3)_2\text{Ph}$, $\text{ReO}_2(\text{CHCMe}_3)(\text{CH}_2\text{CMe}_3)$, $\text{ReO}_2(\text{CHCMe}_3)(\text{CH}_2\text{CMe}_3)(\text{quin})$, and $\text{ReO}_2(\text{CH}_2\text{CMe}_3)(\text{py})_3$ (30 pages). Ordering information is given on any current masthead page. Tables of observed and calculated structure factors can be obtained from the authors.

OM950761O